In situ plasma enhanced atomic layer deposition half cycle study of Al_2O_3 on AlGaN/GaN high electron mobility transistors

Xiaoye Qin and Robert M. Wallace
Department of Materials Science and Engineering, University of Texas at Dallas, Richardson, Texas 75080, USA

(Received 28 May 2015; accepted 19 August 2015; published online 28 August 2015)

A half cycle study of plasma enhanced atomic layer deposited (PEALD) Al_2O_3 on AlGaN is investigated using *in situ* X-ray photoelectron spectroscopy, low energy ion scattering, and *ex situ* electrical characterizations. A faster nucleation or growth is detected from PEALD relative to purely thermal ALD using an H_2O precursor. The remote O_2 plasma oxidizes the AlGaN surface slightly at the initial stage, which passivates the surface and reduces the OFF-state leakage. This work demonstrates that PEALD is a useful strategy for Al_2O_3 growth on AlGaN/GaN devices. [http://dx.doi.org/10.1063/1.4929818]

Metal insulator semiconductor AlGaN/GaN high electron mobility transistors (MISHEMTs) are promising for power device applications due to a lower leakage current than the conventional Schottky AlGaN/GaN HEMTs.[1–3] Among a large number of insulator materials, an Al_2O_3 dielectric layer, deposited by atomic layer deposition (ALD), is often employed as the gate insulator because of a large band gap (and the resultant high conduction band offset on AlGaN[4]), high breakdown field, conformal growth, and a relatively high dielectric constant.[5–7] In the past decade, much work has been done to study the device performance, as well as the interface chemistry for Al_2O_3/AlGaN/GaN MISHEMTs.[5,6,8–17] Although an ALD Al_2O_3 insulator layer grown by Tri-Methyl-Aluminum (TMA) and H_2O precursors decreases the leakage current significantly, the ALD Al_2O_3 is not effective in the passivation of the native AlGaN surface or reduction of the interface state density (D_{it}).[5,12,18] Moreover, due to a high density of positive charges at the AlGaN surface, an undesirable negative threshold voltage shift appears after the ALD Al_2O_3.[6] Recently, numerous reports support that the oxidation of AlGaN can decrease the positive interface charges as well as the D_{it}.[18–25] Our recent work also demonstrates that a remote O_2/N_2 plasma exposure at 550 °C is an available passivation method prior to ALD Al_2O_3.[18] In contrast, O_2 plasma pretreatments under different conditions (flow, time, temperature, etc.) may result in surface damage and a threshold voltage instability ($\Delta V > 1$ V).[26] It is well known that plasma enhanced atomic layer deposition (PEALD) can grow an oxide layer using an oxygen plasma to replace the H_2O precursor.[27–29] Recently, work by Meunier *et al.* shows that PEALD Al_2O_3 is able to enhance device performance.[16,20] However, whether this improvement is relative to the surface oxidation or the Al_2O_3 film is unclear. In this work, a comparison of purely thermal ALD and PEALD is performed to investigate the impact of the O_2 plasma ambient on the AlGaN surface using *in situ* X-ray photoelectron spectroscopy (XPS) and low energy ion scattering (LEIS). *Ex situ* Capacitance-Voltage (C-V) and Current-Voltage (I-V) measurements are exploited to evaluate the associated device performance.

Undoped (0001) $Al_{0.25}Ga_{0.75}N$ samples (30 nm), grown on a 1.2 μm GaN layer on a p-type Si(111) substrate by metal organic chemical vapor deposition (see the wafer structure in Fig. S1(a) in the supplementary material[30]), were obtained from DOWA Electronics Materials (Tokyo, Japan). The samples were first solvent cleaned in acetone, methanol, and isopropanol for one minute each. These samples were then immediately mounted to a sample plate and introduced into an ultra-high vacuum (UHV) system, described in detail elsewhere,[31] which consists of a number of vacuum chambers interconnected by a UHV transfer tube, maintained at $<5 \times 10^{-10}$ mbar. This configuration enables the study of *in situ* surface treatments, thin film depositions, and surface characterization without exposure to atmospheric conditions, preventing spurious surface contamination.

In order to monitor the growth and reaction of Al_2O_3 on the AlGaN surface, XPS was carried out after specific points in the study: (a) after loading the samples to UHV, (b) upon exposing the samples to an atomic layer deposition reactor (Picosun PR200 PEALD reactor (Masala, Finland) operated under purely thermal or plasma-enhanced modes for comparison) for 30 min of annealing (300 °C and 200 °C for ALD and PEALD, respectively, consistent with the following deposition temperature), and (c) after each individual "half cycle"[14,32] pulse of the ALD/PEALD process up to two full cycles. Specifically, the samples were first exposed to one pulse of TMA in the reactor and interrogated with XPS, then transferred back to the PEALD reactor and exposed to one pulse of H_2O (ALD) or remote O_2 plasma (PEALD) prior to again being examined with XPS. The samples were also examined with XPS after 5, 10, 20, and 100 full cycles. *In situ* LEIS was also performed on the sample surface after 20 cycles.

In this study, one full thermal ALD sequence is 0.1 s TMA + 6s Ar Purge + 0.1s H_2O +4s Ar Purge, and the deposition temperature was 300 °C; one full PEALD cycle sequence is 0.1 s TMA + 6 s Ar purge + 28 s remote O_2 plasma + 4 s Ar purge, and the deposition temperature was 200 °C. The remote O_2 plasma was generated by 160 sccm O_2 flow at 2.75 kW. High purity (99.9999%) Ar was used as the precursor carrier and purging gas. The base pressure of the reactor was ~5 mbar.

The XPS was carried out using a monochromated Al kα ($h\nu = 1486.7$ eV) X-ray source, equipped with a 7 channel

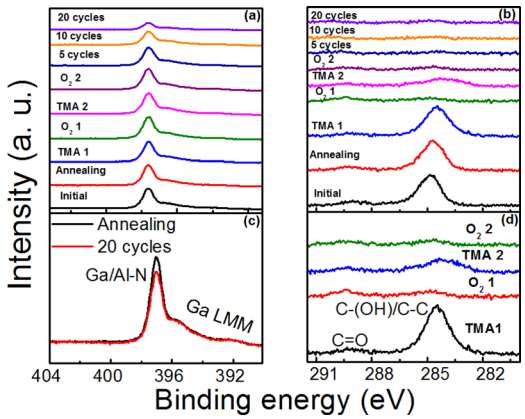

FIG. 1. *In situ* XPS spectra of (a) N 1*s*/Ga *LMM* and (c) C 1*s* core levels from the initial surface, after annealing at 200 °C and each ALD half or full cycle, as indicated. (b) N 1*s*/Ga *LMM* spectra normalized to the Ga *LMM* feature after annealing and after 20 cycles of PEALD Al_2O_3. (d) C 1*s* spectra from the first two cycles of PEALD indicating the initial stage of PEALD Al_2O_3 and its impact on AlGaN surface.

analyzer, using a pass energy of 15 eV, with all scans taken at 45° with respect to the sample normal. Spectra were taken of the Ga $2p_{3/2}$, Ga 3*d*, N 1*s*, Al 2*p*, O 1*s*, and C 1*s* core level regions. XPS peak deconvolution was carried out using an AAnalyzer software with a detailed peak fitting procedure described elsewhere.[14,33] All peaks were referenced to the N 1*s* peak at 397.0 eV to compensate for any shifts in the peak core level positions due to band bending. The LEIS was carried out using the same 7 channel analyzer with biasing conditions suitable for ion detection, and He^+ ions excited by an ISE 100 fine focus ion gun using 1 kV bias and 10 mA emission current.

Additional $\sim 1 \times 1\,cm^2$ AlGaN samples from the same wafer were similarly prepared with subsequent 100 cycles of PEALD Al_2O_3 (for a nominal Al_2O_3 thickness of ~10 nm verified by *ex situ* ellipsometry carried on 100 cycles of Al_2O_3 on Si reference samples) for device fabrication. The fabrication process is described in the supplementary material.[30] The schematic diagrams and geometry details of MOS diodes and transistors are also depicted in Figs. S1(b) and S1(c) in the supplementary material, respectively.[30] C-V measurements were performed on the diodes by an Agilent 4284 LCR meter with a step of 0.2 V and AC modulation voltage of 50 mV with sweep frequencies varying from 5 to 400 kHz. I-V measurements were carried out using a Keithley 4200. All C-V and I-V characterizations were performed in the dark to avoid the influence of photoionization of trapped electrons.[34]

The N 1*s* and Ga *LMM* Auger spectra for each individual step are shown in Fig. 1(a). Ga/Al-N bonding (397.0 eV) and the Ga $L_2M_{45}M_{45}$ Auger feature (spanning ~ 392–398 eV) are detected. After 20 cycles of PEALD Al_2O_3, the intensities of N 1*s* and Ga *LMM* decrease by ~65% due to the attenuation of the overlying Al_2O_3 film. In order to understand chemical states of nitrogen clearly, the N 1*s* and Ga *LMM* spectra after annealing and after 20 cycles of PEALD Al_2O_3 are shown in Fig. 1(b). There is no evidence of detectable Ga-ON (~398 eV) or N-O (~402 eV) bonding, which results in undesirable defects on AlGaN according to our previous *in situ* O_2 plasma pretreatment work.[12] The N 1*s*/Ga *LMM* ratio decreases slightly after 20 cycles of Al_2O_3 because of a formation of surface Ga/Al oxide, and will be further discussed in the Ga $2p_{3/2}$ and Al 2*p* spectra below.

The C 1*s* spectra for each individual step are shown in Fig. 1(c). For the initial starting surface, C=O (~290 eV) and C-(O)H/C-C (~284.5 eV) bonds are detected. The *in situ* 200 °C annealing is not effective at removing the carbon concentration, consistent with our previous work.[14,32] In order to observe the initial reaction between the AlGaN surface and TMA/O_2 plasma, the C 1*s* spectra for the first two full ALD cycles (four half cycles) are also shown in Fig. 1(d). After the first pulse of TMA, the carbon concentration does not increase. Upon exposure to the first pulse of the O_2 plasma (28 s), the C 1*s* peaks, especially the C(O)H/C-C concentration, decreases significantly while the intensity of the C=O feature does not change. After the second pulse of TMA, the C 1*s* peak at ~284.5 eV corresponding to Al-CH_3 binding clearly appears. This behavior indicates that the first pulse of O_2 plasma changes the AlGaN surface, which provides nucleation sites for the following TMA precursor. After the second pulse of O_2 plasma, the C 1*s* peaks corresponding to C-H bonds decrease again, suggesting the removal of CH_3 and a full cycle of TMA/O_2 plasma reaction. The carbon concentration after 20 cycles of PEALD is below XPS detection limits, suggesting a complete reaction with minimized carbon incorporation.

Fig. 2(a) presents the normalized and deconvoluted Ga $2p_{3/2}$ spectra for each individual deposition stage, and shows two peaks indicative of Ga-N bonding from the substrate and Ga-O bonding at the surface. In our work, Ga $2p_{3/2}$ spectra are commonly used due to the superior surface sensitivity (and signal intensity) of the Ga $2p_{3/2}$ spectra relative to other Ga spectral peaks produced using the Al Kα ($h\nu = 1486.7$ eV) source.[35] The fitting parameters are consistent with our previous reports.[10,12,14,18,32] The ratio of the Ga-O to Ga-N peak area (intensity) for the PEALD Al_2O_3 is plotted in Fig. 2(b). As a reference, the ratio of the Ga-O/Ga-N peak areas for the ALD Al_2O_3 is also plotted in Fig. 2(b). The first pulse of TMA does not change the Ga-O concentration. An obvious increase of Ga-oxide is detected after the first pulse of O_2 plasma, but not after the first H_2O precursor as shown in Fig. 2(b). This indicates that the remote plasma oxygen

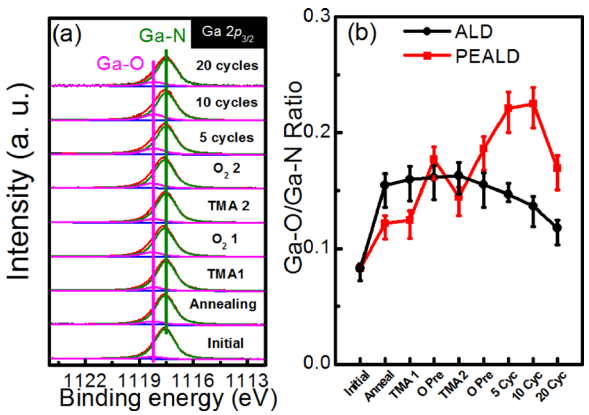

FIG. 2. (a) *In situ* XPS spectra of Ga $2p_{3/2}$ core levels from the initial surface, after annealing in 200 °C, and each individual ALD half cycle. (b) The area ratio of Ga-O/Ga-N from Ga $2p_{3/2}$ shows the change of Ga-oxide concentration during half cycle of ALD and PEALD.

exposure oxidizes the AlGaN surface. Upon exposure to the second pulse of TMA, the Ga-O peak decrease is likely due to the formation Ga-O-Al bonding at the surface.[10] The final Ga-O/Ga-N intensity ratios are ~11.7 ± 1.5% and 16.9 ± 1.9% for ALD and PEALD Al_2O_3, respectively. If we assume that the surface oxide layer consists of 75% Ga_2O_3 and 25% Al_2O_3, the thickness of the Ga/Al oxide layers after 20 cycles of ALD Al_2O_3 and PEALD are both less than 0.1 nm based on the intensity attenuation of the N 1*s* peak, which is below the monolayer (~0.26 nm) coverage. In summary, the PEALD process slightly increases the oxide concentration at the surface relative to the ALD process.

The Al 2*p* spectra for each individual stage in PEALD are shown in Fig. 3(a), which is a direct monitor of the growth of Al_2O_3. The ratio of Al-O to Al-N during the half cycle PEALD is shown in Fig. 3(b) and the ratio of the Al-O/Al-N for each stage during ALD of Al_2O_3 is also shown. The detection of the Al-N bulk peak at 73.5 eV, as well as Al_2O_3 at 74.4 eV, is noted.[14,32] Due to the low binding energy of Al 2*p* core level, the intensity of Al-O bond from the substrate is less prominent compared to the detection of Ga-O from the surface sensitive Ga $2p_{3/2}$ core level.[4,10,12,14,18,32] Consistent with Ga $2p_{3/2}$ spectra, the Al-O bond increases slightly after annealing and the first pulse of O_2 plasma. Importantly, the intensity ratio for PEALD increases faster than the ALD process, indicating the nucleation or growth of PEALD Al_2O_3 on AlGaN is more facile than ALD. It should be noted that measured Al_2O_3 growth rates on Si substrate for ALD and PEALD are 1.14 ± 0.01 and 1.13 ± 0.01 Å/cycle, respectively, suggesting that the difference of growth rates could be ignored here. The thickness of the PEALD Al_2O_3 after 20 cycles on AlGaN is ~1.4 nm according to the attenuation of Ga $2p_{3/2}$ peak area. In contrast, the thickness of ALD Al_2O_3 is ~1.0 nm after 20 cycles. Thus, the relatively enhanced growth is due to Ga/Al-oxide formation (which are reactive nucleation sites for the TMA precursor) after the O_2 plasma exposure, likely coupled with the removal of carbon contamination, which may mitigate the reaction between the AlGaN surface and the TMA precursor.[10] Additionally, a much better coverage of Al_2O_3 by PEALD is demonstrated by *in situ* LEIS, which is sensitive to only the outmost exposed atomic layers on the surface.[36] As Fig. 3(c) shows, no Ga peak is detected while an obvious Ga peak (815 eV) is found with 20 cycles of ALD Al_2O_3 on AlGaN, suggesting that the PEALD Al_2O_3 results in the complete coverage at the initial stage. Moreover, the higher Al peak from the ALD Al_2O_3 sample relative to the PEALD Al_2O_3 is also due to the uncovered AlGaN surface. The stoichiometry of the ALD Al_2O_3 and the PEALD is the same within detectable limits (see Fig. S2 in the supplementary material[30]). The detection of a small fluorine (F) peak is noted and is due to decomposition of reactor elastomer seals. The concentration of F is below XPS detection limits and does not affect the discussion here.

The frequency-dependent C-V curves from 5 kHz to 400 kHz at room temperature are measured to evaluate the interface quality. These C-V curves from diode structures incorporating ALD Al_2O_3 and PEALD Al_2O_3 dielectric layers are shown in Figs. 4(a) and 4(b), and reveal a standard two-step C-V feature.[12,18] Capacitance values for diodes at the plateau where the two dimension electron gas (2DEG) forms are 194 and 196 nF/cm^2 for ALD and PEALD, respectively, consistent with the ~10 nm Al_2O_3/AlGaN stack capacitance.[4] Obvious frequency dependence of capacitance dispersion is detected for both diodes upon further gate bias, corresponding to a high D_{it}. Here, "border trap" (trap states inside the gate insulator but close to the interface) should not be key sources of the D_{it} at the Al_2O_3/AlGaN interface. Our previous work demonstrates that Al_2O_3/AlGaN and HfO_2/AlGaN diodes present a similar level of D_{it}, and AlGaN surfaces have a much more impact on the D_{it}. Long *et al.* also show the absence of border traps for ALD Al_2O_3/GaN interface.[37] The PEALD approach decreases the dispersion slightly. This may be due to the formation of Ga-O, which likely passivates the AlGaN surface.[18] The forward and backward C-V curves at 100 kHz can be seen as insets within Figs. 4(a) and 4(b), and show very small hysteresis values (ΔV):0.09 and 0.13 V for ALD and PEALD Al_2O_3, respectively. It is thought that the PEALD process does not contribute a significant density of slow traps.[12] The gate leakage current densities of Schottky AlGaN/GaN, ALD Al_2O_3/AlGaN/GaN, and PEALD Al_2O_3/AlGaN/GaN are shown in

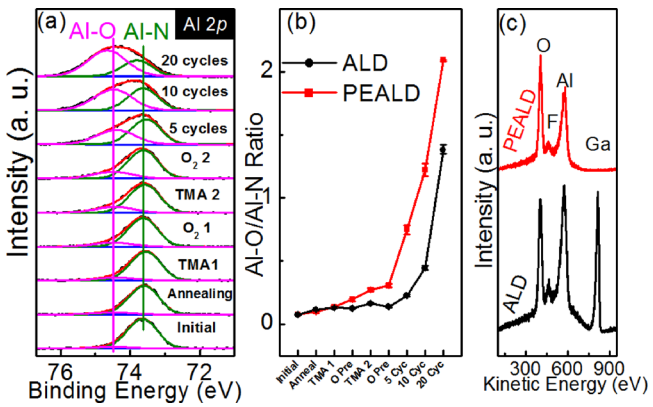

FIG. 3. (a) *In situ* XPS spectra of Al 2*p* core levels from initial surface, after annealing in 200 °C, and each individual ALD half cycle. (b) The ratio of Al-O/Al-N from Al 2*p* peaks during half cycle ALD and PEALD indicating the growth of Al_2O_3. (c) Comparison of LEIS after 20 cycles of ALD to the PEALD Al_2O_3 studied here. (See 25 cycles of ALD Al_2O_3 on AlGaN in Ref. 10.)

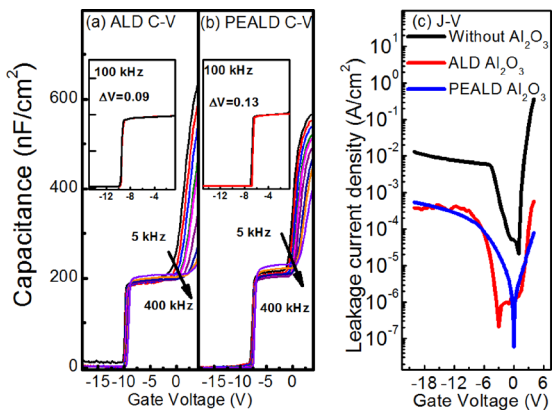

FIG. 4. Comparison of frequency-dependent C-V curves for (a) ALD Al_2O_3/AlGaN/GaN and (b) PEALD Al_2O_3/AlGaN/GaN diodes. Insets show forward and backward C-V curves. (c) Leakage current density-voltage plots for Schottky AlGaN/GaN, ALD Al_2O_3/AlGaN/GaN, and PEALD Al_2O_3/AlGaN/GaN diodes.

Fig. 4(c). Either ALD or PEALD Al_2O_3 layer effectively suppresses the leakage current, consistent with the relatively high conduction band offset (CBO) values in the band diagram (see Figs. S3(c) and S3(f)[30]). It should be noted that the O_2 plasma in the PEALD is well controlled using a relative short exposure time (28 s/per pulse) and a low substrate temperature (200 °C). In contrast, our previous work shows that a 10 min of 300 °C O_2 plasma excited by another RF plasma generator results in a worse frequency dispersion than ALD Al_2O_3/AlGaN/GaN diodes.[18] Therefore, it is essential to control and optimize the O_2 plasma conditions for a specific tool carefully.

The threshold voltage (V_{TH}) values extracted from I_{DS}-V_{DS} curves are −3.9, −10.3, and −9.5 V for HEMTs, ALD-MOSHEMTs, and PEALD-MOSHEMTs, respectively, and the extrapolation methods are included in supplementary material.[30] Obviously, a negative V_{TH} shift is detected from MISHEMTs with Al_2O_3 layer due to a high density of positive charges at the interface, in agreement with our previous work.[4] However, compared to ALD-MISHEMTs, there is a +1 V V_{TH} shift for PEALD-MISHEMTs. The oxidation of AlGaN during PEALD Al_2O_3 likely reduces the positive charge density.[18] The DC characteristics of HEMT and MISHEMTs are plotted in Fig. 5(a). The I_{DS}-V_{DS} output characteristics for all devices present a standard pinch off behavior. The saturation forward and backward I_{DS}-V_{GS} at $V_{DS} = 20$ V curves are shown in Fig. 5(b). Importantly, the PEALD Al_2O_3 layer reduces the OFF-state drain leakage by more than one order of magnitude and improves the I_{ON}/I_{OFF} current ratio. This behavior also reveals that the chemical control of the interface is also critical for the transistor transfer performance. Consistent with the C-V response, no obvious V_{TH} instability is detected.

In conclusion, a high quality Al_2O_3 film is grown on AlGaN/GaN using PEALD, with the faster nucleation rate and better coverage than that obtained through standard, thermal ALD. The remote plasma conditions in the PEALD process result in a slight increase of Al/Ga oxide without formation of Ga/Al-O-N or N-O bonding. According to our previous studies, the formation Ga-O-N, but not Ga-O, is a sign of device degradation.[12,18] The Al/Ga-oxide passivates the AlGaN surface and decreases D_{it} as well as the OFF-state leakage. As expected, the PEALD Al_2O_3 layer reduces the gate leakage current, similar to ALD Al_2O_3. Overall, PEALD Al_2O_3 is an appropriate technology for the Al_2O_3 growth on AlGaN.

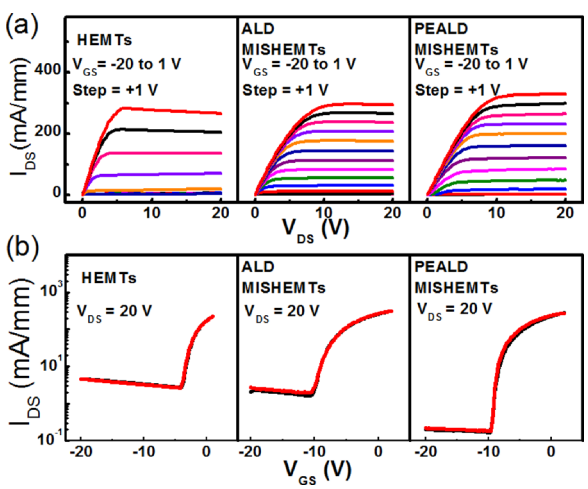

FIG. 5. (a) Output characteristics of HEMTs, ALD-MISHEMTs, and PEALD-MISHEMTs. (b) Transfer characteristics of HEMTs, ALD-MISHEMTs, and PEALD-MISHEMTs indicating a lower OFF-state leakage.

This work was supported by the Asian Office of Aerospace Research and Development (AOARD) through the Air Force office of Scientific Research (AFOSR) under Grant No. FA2386-14-1-4069. The authors thank Dr. J. Kim, Dr. Y. Byun, and Mr. A. Lucero for helpful discussions.

[1]T. Hashizume, S. Ootomo, S. Oyama, M. Konishi, and H. Hasegawa, J. Vac. Sci. Technol. B **19**, 1675 (2001).
[2]M. A. Khan, X. Hu, A. Tarakji, G. Simin, J. Yang, R. Gaska, and M. S. Shur, Appl. Phys. Lett. **77**, 1339 (2000).
[3]U. K. Mishra, P. Parikh, and Y. F. Wu, Proc. IEEE **90**, 1022 (2002).
[4]X. Qin, L. Cheng, S. McDonnell, A. Azcatl, H. Zhu, J. Kim, and R. M. Wallace, J. Mater. Sci. Mater. Electron. **26**, 4638 (2015).
[5]S. Yang, Z. Tang, K. Wong, Y. Lin, C. Liu, Y. Lu, S. Huang, and K. J. Chen, IEEE Electron Device Lett. **34**, 1497 (2013).
[6]M. Ťapajna, M. Jurkovič, L. Válik, Š. Haščík, D. Gregušová, F. Brunner, E.-M. Cho, T. Hashizume, and J. Kuzmík, J. Appl. Phys. **116**, 104501 (2014).
[7]G. D. Wilk, R. M. Wallace, and J. M. Anthony, J. Appl. Phys. **89**, 5243 (2001).
[8]T. Hashizume, S. Anantathanasarn, N. Negoro, E. Sano, H. Hasegawa, K. Kumakura, and T. Makimoto, Jpn. J. Appl. Phys., Part 2 **43**, L777 (2004).
[9]M. Capriotti, A. Alexewicz, C. Fleury, M. Gavagnin, O. Bethge, D. Visalli, J. Derluyn, H. D. Wanzenböck, E. Bertagnolli, D. Pogany, and G. Strasser, Appl. Phys. Lett. **104**, 113502 (2014).
[10]X. Qin, H. Dong, B. Brennan, A. Azacatl, J. Kim, and R. M. Wallace, Appl. Phys. Lett. **103**, 221604 (2013).
[11]M. Van Hove, X. Kang, S. Stoffels, D. Wellekens, N. Ronchi, R. Venegas, K. Geens, and S. Decoutere, IEEE Trans. Electron Devices **60**, 3071 (2013).
[12]X. Qin, A. Lucero, A. Azcatl, J. Kim, and R. M. Wallace, Appl. Phys. Lett. **105**, 011602 (2014).
[13]X.-H. Ma, J.-J. Zhu, X.-Y. Liao, T. Yue, W.-W. Chen, and Y. Hao, Appl. Phys. Lett. **103**, 033510 (2013).
[14]B. Brennan, X. Qin, H. Dong, J. Kim, and R. M. Wallace, Appl. Phys. Lett. **101**, 211604 (2012).
[15]R. Lossy, H. Gargouri, M. Arens, and J. Wuürfl, J. Vac. Sci. Technol. A **31**, 01A140 (2013).
[16]R. Meunier, A. Torres, and M. Charles, ECS Trans. **58**, 269 (2013).
[17]K.-Y. Park, H.-I. Cho, J.-H. Lee, S.-B. Bae, C.-M. Jeon, J.-L. Lee, D.-Y. Kim, C.-S. Lee, and J.-H. Lee, Phys. Status Solidi **7**, 2351 (2003).
[18]X. Qin, H. Dong, J. Kim, and R. M. Wallace, Appl. Phys. Lett. **105**, 141604 (2014).
[19]H.-Y. Liu, C.-S. Lee, W.-C. Hsu, L.-Y. Tseng, B.-Y. Chou, C.-S. Ho, and C.-L. Wu, IEEE Trans. Electron Devices **60**, 2231 (2013).
[20]R. Meunier, A. Torres, E. Morvan, M. Charles, P. Gaud, and F. Morancho, Microelectron. Eng. **109**, 378 (2013).
[21]N. Harada, Y. Hori, N. Azumaishi, K. Ohi, and T. Hashizume, Appl. Phys. Express **4**, 021002 (2011).
[22]F. Roccaforte, F. Giannazzo, F. Iucolano, C. Bongiorno, and V. Raineri, J. Appl. Phys. **106**, 023703 (2009).
[23]S. Huang, X. Liu, K. Wei, G. Liu, X. Wang, B. Sun, X. Yang, B. Shen, C. Liu, S. Liu, M. Hua, S. Yang, and K. J. Chen, Appl. Phys. Lett. **106**, 033507 (2015).
[24]D. Gregušová, M. Jurkovič, Š. Haščík, M. Blaho, A. Seifertová, J. Fedor, M. Ťapajna, K. Fröhlich, P. Vogrinčič, J. Liday, J. Derluyn, M. Germain, and J. Kuzmik, Appl. Phys. Lett. **104**, 013506 (2014).
[25]L.-H. Huang, S.-H. Yeh, C.-T. Lee, H. Tang, J. Bardwell, and J. B. Webb, IEEE Electron Device Lett. **29**, 284 (2008).
[26]S. Ozaki, T. Ohki, M. Kanamura, T. Imada, N. Nakamura, N. Okamoto, T. Miyajima, and T. Kikkawa, in *international Conference Compd. Semicond. Manuf. Technol. Digest*, Boston, MA, 23-26 April 2012, paper 11a.1, availabe at http://gaasmantech.com/Digest/2012/papers/11a.1.087.pdf.
[27]S. M. George, Chem. Rev. **110**, 111 (2010).

[28]B. Hoex, S. B. S. Heil, E. Langereis, M. C. M. Van De Banden, and W. M. M. Kessels, Appl. Phys. Lett. **89**, 042112 (2006).
[29]J. W. Lim and S. J. Yun, Electrochem. Solid-State Lett. **7**, F45 (2004).
[30]See supplementary material at http://dx.doi.org/10.1063/1.4929818 for additional device fabrication, band diagrams and the extraction of threshold voltage.
[31]R. M. Wallace, ECS Trans. **16**, 255 (2008).
[32]X. Qin, B. Brennan, H. Dong, J. Kim, C. L. Hinkle, and R. M. Wallace, J. Appl. Phys. **113**, 244102 (2013).
[33]A. Herrera-Gómez, A. Hegedus, and P. L. Meissner, Appl. Phys. Lett. **81**, 1014 (2002).
[34]*Materials and Reliability Handbook for Semiconductor Optical and Electron Devices*, edited by O. Ueda and S. J. Pearton (Springer, New York, 2013), pp. 147–205.
[35]C. L. Hinkle, M. Milojevic, E. M. Vogel, and R. M. Wallace, Appl. Phys. Lett. **95**, 151905 (2009).
[36]F. Zhang, B. King, and D. O'connor, Phys. Rev. Lett. **75**, 4646 (1995).
[37]R. D. Long, A. Hazeghi, M. Gunji, Y. Nishi, and P. C. McIntyre, Appl. Phys. Lett. **101**, 241606 (2012).

In Situ Plasma Enhanced Atomic Layer Deposition Half Cycle Study of Al_2O_3 on AlGaN/GaN High Electron Mobility Transistors

Citation:

Qin, X., and R. M. Wallace. 2015. "In situ plasma enhanced atomic layer deposition half cycle study of Al_2O_3 on AlGaN/GaN high electron mobility transistors." Applied Physics Letters 107(8), doi: 10.1063/1.4929818